

# Chapter 12

## Arrested Compression Tests on Two Types of Sand

Eduardo Suescun-Florez, Stephan Bless, Magued Iskander, and Camilo Daza

**Abstract** Silica sand and quartz sand were subjected to uniaxial loading and unloading at rates of 0.1/s and 0.0001/s. The particle size distribution was measured, and found to be significantly altered when peak strains were 10 % or greater. The loading modulus for silica sand was bilinear, and suggestive of elastic-plastic behavior, where the plastic part is due to void closure. On unloading, the modulus is close to the loading “elastic” value. Coral sand is softer than silica sand on loading, and the modulus is almost constant and much less than for silica sand. Both types of sand are recovered with a higher density than can be obtained with the starting particle mix. This suggests particles have crushed and filled some of the voids. Indeed, reduction of mean particle size is verified from post-test analysis. Coral sand, which has the greater reduction in void content, also exhibits increased particle breakup.

**Keywords** Silica sand • Coral sand • Confined compression • Crushing • Porosity

### 12.1 Introduction

Particle breakage is important for understanding the constitutive mechanisms in sand [1]. Breakage progresses in a number of stages starting with damage, followed by crushing, and possibly reaching complete pulverization of the grains which is also known as comminution. At all stages, particle breakage influences the macroscopic stress–strain behavior and permeability of sand especially at high pressures. [2, 3]. The role of particle breakage on the constitutive behavior of sand has been investigated by different means including breakage indices ([4, 5]. Other studies have correlated vertical stresses with pore volume reduction [6]. At high vertical stresses the behavior may be described using parallel normal compression and critical state lines, both of which are related to the degree of particle damage [7].

The main goal of this paper was to assess the evolution of particle damage of two natural sands subjected to one dimensional compression loading. Strain-controlled tests were arrested between 5 and 30 % strain. Evolution of crushing was assessed when post-tests samples were subjected to dynamic imaging techniques.

### 12.2 Materials Tested

Two sands were selected for investigation, a silica sand and a coral sand. The two sands were selected mainly for the difference in their grain strength, which is attributed to the different mineralogical compositions. The physical properties of the tested sands are summarized below. More information of these two materials can be found in [8].

Silica sand, was named #1-Dry by its distributor US Silica. Particles are sub-rounded to sub-angular with medium to high sphericity having diameters ranging from 10 to 800  $\mu\text{m}$ , and aspect ratio values between 0.6 and 0.75. The mean particle size (D50) was found to be 340  $\mu\text{m}$  and the coefficient of uniformity was determined as 1.59. The material is poorly graded and classified as SP according to ASTM’s Unified Soil Classification System (USCS). The specific gravity of the grains was 2.66. Maximum and minimum densities were determined following standards [9, 10], and were found to be 1.84 and 1.43  $\text{g}/\text{cm}^3$  respectively, corresponding to porosity of 30 % and 45 %, respectively.

Coral sand labeled with the commercial name Carib Sea was purchased from an aquarium store. It was crushed in a grinder and separated into different grain size ranges. These particles are sub-rounded and less angular than those of the

---

E. Suescun-Florez • S. Bless (✉) • M. Iskander • C. Daza  
Tandon School of Engineering, New York University, 6 Metrotech Center, Brooklyn, NY 11201, USA  
e-mail: [sbless@nyu.edu](mailto:sbless@nyu.edu)

silica sand. Particles size varies from 10 to 1500  $\mu\text{m}$  exhibiting aspect ratios around 0.70. The mean particle size (D50) was found to be 615  $\mu\text{m}$  and the coefficient of uniformity was 1.92. The material is poorly graded and is classified as SP according to the USCS. Specific gravity of the grains is 2.65, and its maximum and minimum densities are 1.81 and 1.55  $\text{g}/\text{cm}^3$  respectively; corresponding porosities were 32 % and 42 % respectively.

### 12.3 Arrested Testing Technique

Uniaxial compression tests were conducted on cylindrical samples of dry sand having a diameter 76.2 mm and thickness of 12.7 mm, corresponding to an aspect ratio of six. Chambers were lubricated before being filled with sand to minimize side friction on the cell boundary. Samples were prepared with an approximate relative density of 85 %, corresponding to initial porosities of 32 % and 33 % for silica and coral sand. The compression was arrested at 5, 15, or 25 % strain, and then samples were unloaded.

Once uniaxial tests were complete, all material was retrieved, and particle size and shape analysis were performed on the entire sample using a QuicPic dynamic image particle analyzer. The particle analyzer provides a particle detection limit of 10  $\mu\text{m}$ .

### 12.4 Stress-Strain Behavior of Sands

Results from uniaxial compression tests arrested at 5, 15, and 20–25 % strain for silica sand are shown in Fig. 12.1, and coral sand in Fig. 12.2. Solid lines correspond to high strain rate (0.1/s) whereas dashed lines show the behavior at low strain rate (0.0001/s).

Since the deformation is uniaxial, the strain is equal to the change specific volume divided by the initial specific volume. Hence density is related to strain by

$$\rho = \rho_0 / (1 - \varepsilon) \quad (12.1)$$

Since the moduli of void-free polycrystalline quartz (e.g. quartzite) or coral skeletons are orders of magnitude higher than the modulus of these sands, we can assume all of the change in density is due to removal of porosity,  $n$ , hence

$$n = 1 - \rho / \rho_{00} \quad (12.2)$$

where  $\rho_0$  and  $\rho_{00}$  are initial test density and grain density, respectively. Figure 12.3 shows stress vs. porosity for the 20 % peak strain case at the higher strain rate for both materials.

For silica sand, the loading modulus appears to be bilinear and increases with strain rate. Unloading moduli are near constant and have less rate dependence. It is interesting that there is substantial increase in porosity during unloading. After the load/unload cycle the density has increase to about 2  $\text{g}/\text{cm}^3$ . In other uniaxial experiments [8] the modulus also decreased with strain however the transition between initial and final modulus was difficult to resolve. In other words, there are three behaviors in the load-unload curves for silica sand which probably correspond to different micromechanical deformation

**Fig. 12.1** Stress-strain data from arrested tests in silica sand

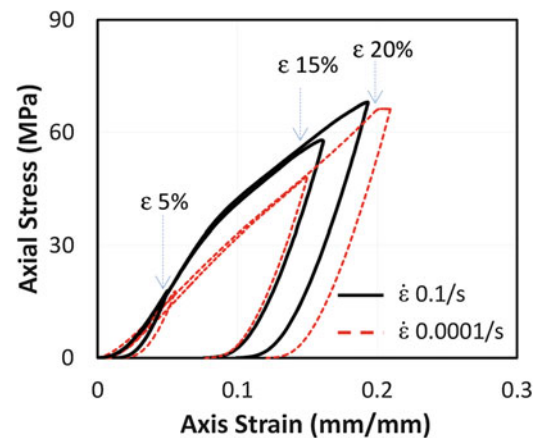


**Fig. 12.2** Stress–strain data from arrested tests in coral sand

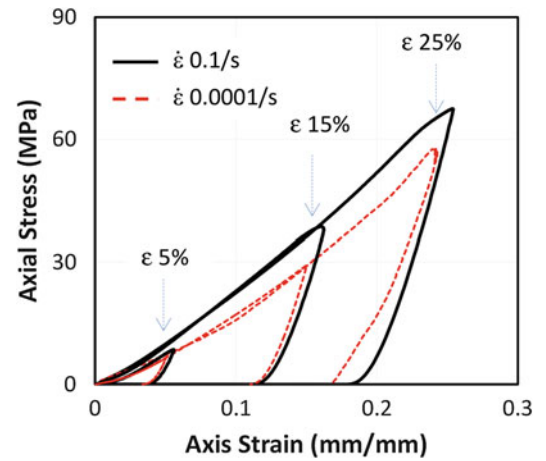
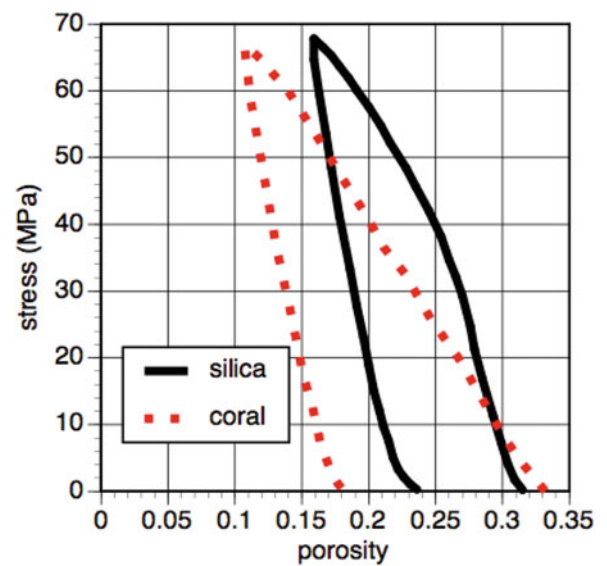


**Fig. 12.3** Stress–porosity data from silica sand and coral sand tests unloaded from 20 % strain



mechanisms. After a short ramp due to seating, the stress increases linearly with strain, with a modulus of about 550 MPa at the higher strain rate. At about 9 % strain the modulus softens but thereafter remains nearly constant at about 280 MPa. Unloading occurs with a nearly linear modulus which is commensurate with that of the initial loading, about 1100 MPa, except at the end.

At the peak strain of each test, the secant modulus (0 to peak stress) increases about 10 % as the strain rate is increased by three orders of magnitude. This rate dependence of the loading modulus is consistent with that observed previously in [8], although the modulus values there are slightly stiffer than seen in these tests.

The only reversible process active in sand is presumably elastic deformation of grains as they shift position. This mechanism is probably responsible for the initial modulus and the unloading modulus. Inelastic mechanisms could include frictional sliding, irreversible closing of voids, and crushing to produce small particles that can fill the gaps between larger particles. The porosity after the load/unload cycle from 20 % strain is 24 %, which is less than the lowest porosity that could be observed in the starting material. This indicates that some material has been crushed, which was verified (see below) with the particle size analyzer.

The stress/strain curve appears to be very similar to an elastic-plastic shock compression curve, which is also for 1-D strain. If we apply that interpretation to these data, then the initial loading represents elastic compression in which the modulus is  $K + 4G/3$ , and the higher-stress part is volumetric compression without additional shear strain, for which the modulus is  $K$ . The hypothesis that the upper modulus is associated with volumetric collapse is supported by the observation that the difference in porosity between the initial and unloaded sample is about equal to the change in porosity during the “plastic” part of the compression curve. However, whether or not this is correct for silica sand should still be considered speculative.

For coral sand, loading takes place with a continuously stiffening modulus. Unloading takes place with a nearly constant modulus that does not vary with strain. The unloading modulus is much stiffer than the loading modulus. Loading moduli stiffen with strain rate, but unloading moduli do not. The unloading modulus, between about 50 and 20 MPa of axial stress, is 1000 MPa. This is remarkably close to the unloading modulus of quartz sand. It seems that the unloading moduli of these granular materials has little to do with the intrinsic properties of the grains themselves. Given that the unloading modulus is so much greater than the loading modulus, it appears that most of the loading behavior must be inelastic in coral sand. Because of the large hysteresis between the loading and unloading moduli, substantially greater porosity is removed by the load/unload cycle in coral sand than for silica sand. As was the case with silica sand, the final porosity is less than the porosity of the initial material at its maximum density; therefore, some void volume must be filled with crushed material.

## 12.5 Particle Damage

The material recovered from arrested tests was subjected to size analysis via dynamic imaging techniques. Results are shown in Fig. 12.4 for both types of sand. At 5 % strain there is little change in the particle size distribution. Reduction in particle sizes is evident at 10 and 20 % peak strain.

The degree of particle size reduction from 10 to 20 % peak strain was higher at the higher strain rate. Surprisingly, it was also observed that when either sand fractures, particles preserve similar aspect ratios to that of the parent material. The effect is more consistent as the applied strain increases.

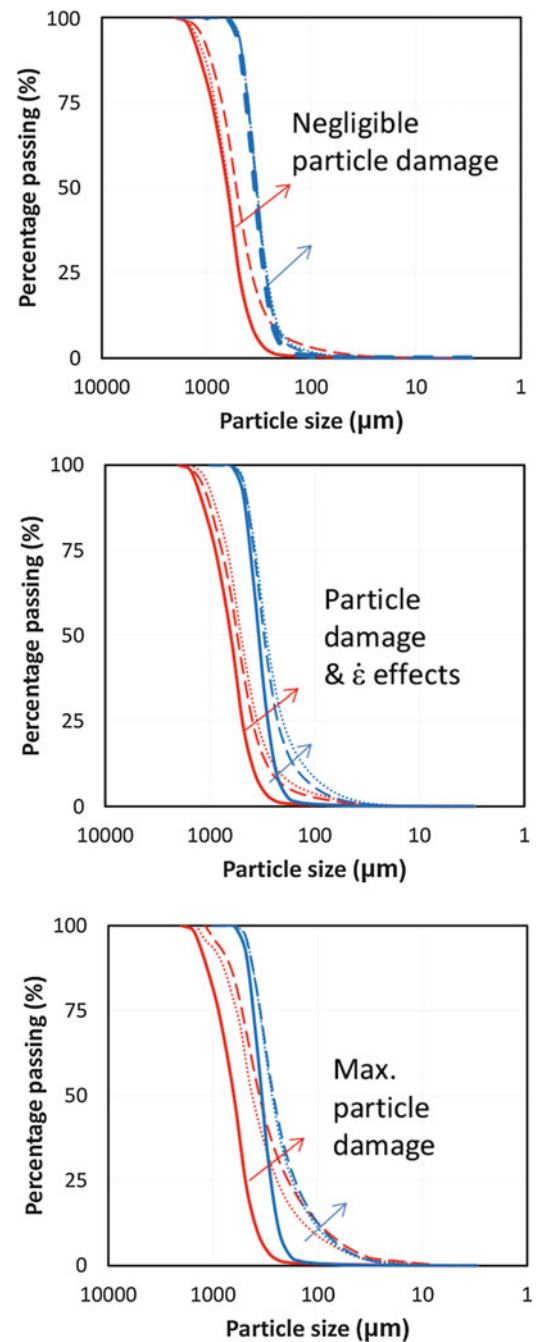
Particle damage was greater in coral sand. For example, consider the initial median particle size. After 20 % strain 85 % of the coral sand particles were less than the initial median size, whereas in silica sand, only 70 % were smaller than the median. The small particles can fit between the large ones, which explains why the porosity decreases was greater in coral sand than in silica sand.

## 12.6 Conclusions

Load-unload-recovery compression tests on sand display characteristics that are specific to particle composition, but also characteristics that appear insensitive to particle composition. Loading of silica sand to 60 MPa results in a bilinear stress strain curve suggestive of elastic-plastic behavior. On unloading, the modulus is close to the loading “elastic” value. Coral sand is softer than silica sand on loading, and the modulus is almost constant and much less than for silica sand. However, the unloading modulus is very similar to silica sand. This may indicate that the particle rearrangement that occurs on unloading is relatively independent of the grain properties. All materials end up at a higher density than can be obtained with the starting particle mix. This suggests particles have crushed and filled some of the voids. Indeed, reduction of mean particle size is verified from post-test analysis. Coral sand, which has the greater reduction in void content, also exhibits increased particle breakup.

**Acknowledgment** The authors gratefully acknowledge the support of the Defense Threat Reduction Agency Grant No: HDTRA1-10-1-0049 and The United States National Science Foundation Grant No: DGE 0741714.

**Fig. 12.4** Particle size distributions from original material and arrested tests. *Upper: 5 % strain. Middle: 10 % strain. Lower: 25 or 30 % strain. Blue curves: silica. Red curves: coral*



## References

1. Russell, A.R., Einav, I.: Energy dissipation from particulate systems undergoing a single particle crushing event. *Granul. Matter* **15**(3), 299–314 (2013)
2. Lade, P.V., Yamamuro, J.A., Bopp, P.A.: Significance of particle crushing in granular materials. *J. Geotech. Eng.* **122**(4), 309–316 (1996)
3. Shahnazari, H., Rezvani, R.: Effective parameters for the particle breakage of calcareous sands: An experimental study. *Eng. Geol.* **159**, 98–105 (2013). doi:[10.1016/j.enggeo.2013.03.005](https://doi.org/10.1016/j.enggeo.2013.03.005)
4. Hardin, B.O.: Crushing of soil particles. *J. Geotech. Eng. ASCE* **111**, 1177–1192 (2007)
5. Lee, K.L., Farhoomand, I.: Compressibility and crushing of granular soil in anisotropic triaxial compression. *Can. Geotech. J.* **4**(1), 68–86 (1967)
6. McDowell, G.R., Bolton, M.D.: On the micromechanics of crushable aggregates. *Geotechnique* **48**(5), 667–679 (1998)
7. Coop, M.R., Lee, I.K.: The behavior of granular soils at elevated stresses. In: Housley, G.T., Schofield, A.N. (eds.) *Predictive Soil Mechanics*, pp. 186–199. Thomas Telford, London (1993)

8. Suescun-Florez, E., Kashuk, S., Iskander, M., Bless, S.: Predicting the uniaxial compressive response of granular media over a wide range of strain rates using the strain energy density concept. *J. Dyn. Behav. Mater.* **1–17** (2015)
9. ASTM D. 4253-14: Standard Test Methods for Maximum Index Density and Unit Weight of Soils Using a Vibratory Table. ASTM International, West Conshohocken (2014). [www.astm.org](http://www.astm.org)
10. ASTM D. 4254-14: Standard Test Methods for Minimum Index Density and Unit Weight of Soils and Calculation of Relative Density. ASTM International, West Conshohocken (2014). [www.astm.org](http://www.astm.org)